A linear radio frequency plasma reactor for potential and current mapping in a magnetized plasma

Eric Faudot, Stéphane Devaux, Jérôme Moritz, Stéphane Heuraux, Pedro Molina Cabrera, Frédéric Brochard

▶ **To cite this version:**

Eric Faudot, Stéphane Devaux, Jérôme Moritz, Stéphane Heuraux, Pedro Molina Cabrera, et al.. A linear radio frequency plasma reactor for potential and current mapping in a magnetized plasma. Review of Scientific Instruments, 2015, 86 (6), pp.063502. 10.1063/1.4921905 . hal-04169573

HAL Id: hal-04169573
https://hal.science/hal-04169573

Submitted on 24 Jul 2023

HAL is a multi-disciplinary open access archive for the deposit and dissemination of scientific research documents, whether they are published or not. The documents may come from teaching and research institutions in France or abroad, or from public or private research centers.

L'archive ouverte pluridisciplinaire **HAL**, est destinée au dépôt et à la diffusion de documents scientifiques de niveau recherche, publiés ou non, émanant des établissements d'enseignement et de recherche français ou étrangers, des laboratoires publics ou privés.

AIP | Review of Scientific Instruments

A linear radio frequency plasma reactor for potential and current mapping in a magnetized plasma

E. Faudot, S. Devaux, J. Moritz, S. Heuraux, P. Molina Cabrera, and F. Brochard

Citation: Review of Scientific Instruments **86**, 063502 (2015); doi: 10.1063/1.4921905
View online: http://dx.doi.org/10.1063/1.4921905
View Table of Contents: http://scitation.aip.org/content/aip/journal/rsi/86/6?ver=pdfcov
Published by the AIP Publishing

Articles you may be interested in

Fluid modeling of radio frequency and direct currents in a biased magnetized plasma
Phys. Plasmas **20**, 043514 (2013); 10.1063/1.4802190

Quantitative determination of mass-resolved ion densities in H2-Ar inductively coupled radio frequency plasmas
J. Appl. Phys. **113**, 093304 (2013); 10.1063/1.4794165

Broadening of rectified potential structures induced by rf currents in a magnetized plasma: Application to ITER scrape-off-layer
Phys. Plasmas **17**, 042503 (2010); 10.1063/1.3357334

Spectral and spatial characterization of a radio frequency power absorption in high pressure helicon plasmas
Phys. Plasmas **8**, 4659 (2001); 10.1063/1.1394779

Radio-frequency plasma potential variations originating from capacitive coupling from the coil antenna in inductively coupled plasmas
J. Appl. Phys. **85**, 3428 (1999); 10.1063/1.369700

This article is copyrighted as indicated in the article. Reuse of AIP content is subject to the terms at: http://scitationnew.aip.org/termsconditions. Downloaded to IP: 193.50.135.4 On: Fri, 30 Oct 2015 10:16:52

A linear radio frequency plasma reactor for potential and current mapping in a magnetized plasma

E. Faudot, S. Devaux, J. Moritz, S. Heuraux, P. Molina Cabrera, and F. Brochard
IJL, UMR 7198 CNRS, Universite de Lorraine, 54500 Vandoeuvre les Nancy, France

(Received 2 February 2015; accepted 19 May 2015; published online 8 June 2015)

Langmuir probe measurements in front of high power ion cyclotron resonant frequency antennas are not possible or simply too noisy to be analyzed properly. A linear experiment is a radio frequency (RF) magnetized plasma discharge reactor designed to probe the rectified potential in front of such antennas but at low power level (1 kW) to next improve antenna design and mitigate sheath effects. The maximum magnetic field is 0.1 T, and the RF amplifier can work between 10 kHz and 250 MHz allowing ion cyclotron resonances for argon or helium. The first measurements with no magnetic field are presented here, especially 2D potential maps extracted from the RF compensated probe measurements yield $ni \approx 10^{15}$ m^{-3} and $Te \approx 2$ eV for RF power lower than 100 W. Series resonances in the chamber are highlighted and allow to deduce the plasma parameters from a simple equivalent impedance model of the plasma in helium gas. Next studies will be focused on magnetized plasmas and especially magnetized RF sheaths. © *2015 AIP Publishing LLC.* [http://dx.doi.org/10.1063/1.4921905]

I. INTRODUCTION

Interaction between ICRF (Ion Cyclotron Resonant Frequency) heating devices[1] and the edge plasma lying in the scrape off layer (SOL)[2] of tokamaks is one of the most critical issues for fusion plasma. Large potentials and arcs, arising from high RF (Radio Frequency) power, prevent proper measurements of plasma characteristics in tokamaks, as they degrade the quality of the Langmuir probe data close to the antenna. As a consequence, studying such complicated interactions requires a dedicated device able to diagnose potentials, currents, and heat fluxes induced by a RF antenna.

We designed a low power heating system, within a cylindrical magnetized chamber, which is able to perform accurate measurements (down to 0.1 mm) of the plasma parameters in the vicinity of the RF antenna. Though this kind of reactor is not a new concept, its originality arises from its broadband RF amplifier able to launch RF power up to 600 W. The wide band of achievable frequencies, from 10 kHz to 250 MHz, allows for exciting the ion cyclotron frequency as well as many other resonances in the plasma.

Another innovation of this device is the 3D mapping that can be performed for both potential and current, thanks to a self-compensated RF probe[3] mounted on a 3 dimensional manipulator (made by the Cryoscan company) actuated by step motors (see Fig. 1).

The first part and second part of this paper focuses on a technical description and physics involved in the device, called Aline (A LINear Experiment). The third part presents the first 2D mapping of the floating plasma potential obtained with no magnetic field as well as the deduced plasma parameters. These maps are then compared to analytical and numerical models[4,5] in order to validate the fluid assumptions they rely on. The final part is dedicated to the prospects and expectations from such an experiment.

II. TECHNICAL DESCRIPTION

A. The vacuum chamber

The Aline reactor is a cylindrical chamber (1 m long, 30 cm in diameter, for a thickness of 3 mm) made of 304L stainless steal and equipped with 15 ports arranged according to Figures 2 and 3. This chamber is divided into 2 parts assembled by an iso-K flange with centering O-ring. The longest part of the chamber (70 cm) stands on 2 rails and can be shifted by 50 cm to access the inner chamber so that different antenna designs can easily be fitted inside, for instance. The shortest part (30 cm) is connected to both the manipulator and the turbo molecular pump via a tee.

B. The manipulator

The probe is mounted on a 3 dimension manipulator able to move in a range of 50 cm along the longitudinal axis z and 10 cm along both x and y axes. It is actuated with 10 micrometers accuracy step motors. Such an accuracy is necessary to probe sub-millimeter sheaths in a plasma density within the range 10^{15} to 10^{17} m^{-3} which are the expected densities in Aline. The manipulator is operated by a Labview program able in the same time to trigger the probe acquisition at each motion step.

C. The probe

The Langmuir probe is a RF self-compensated probe avoiding I-V characteristics from being shifted in RF plasmas.[3] This ESPION probe is built by Hiden company. Probing a potential in a RF environment requires to take into account the equivalent impedance of the probing device which can disturb the current and the potential in the plasma. This probe is thus designed to compensate this shifting at frequencies around 13.56 MHz.[6]

 ©2015 AIP Publishing LLC
This article is copyrighted as indicated in the article. Reuse of AIP content is subject to the terms at: http://scitationnew.aip.org/termsconditions. Downloaded to IP: 193.50.135.4 On: Fri, 30 Oct 2015 10:16:52

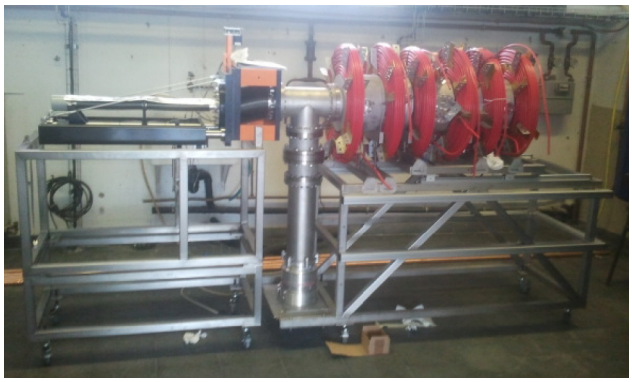

FIG. 1. Picture of the new experimental plasma reactor "Aline." On the left stands the motorized manipulator, in the middle on the ground is the turbo-pump, and on the right the main plasma chamber surrounded by red magnetic coils.

The acquisition can be setup so that each point of a given I-V characteristic actually results from an averaging other multiple measurements, strongly increasing the signal-to-noise ratio.

The probe (Figure 4) can be biased from −200 to +100 volts and collects current up to 1 A on a tungsten cylindrical tip (0.15 mm in diameter and 10 mm long). The main body of the probe is 1.5 m long so that the center of the chamber is reached at half the longitudinal displacement of the manipulator. The main body is made of an aluminum alloy to provide the rigidity needed. The main goal for this probe is to measure the plasma potential to draw a potential map in front of the antenna as it has been done in tokamaks, especially in Tore Supra.[7,8]

D. The magnetic coils and the DC power supply

The coils are composed of 75 turns of copper tube (6 by 8 mm in diameter) insulated with a 1 mm polyvinyl chloride (PVC) layer. The inner radius of these coils is equal to the chamber radius (150 mm) and the outer radius is 320 mm for a longitudinal width of 50 mm. Six coils are positioned along the chamber to create a 0.1 T magnetic field under 200 A per coil. The corresponding magnetic field profile appears in Figure 5. The theoretical resistance of each coil is 0.08 ohm

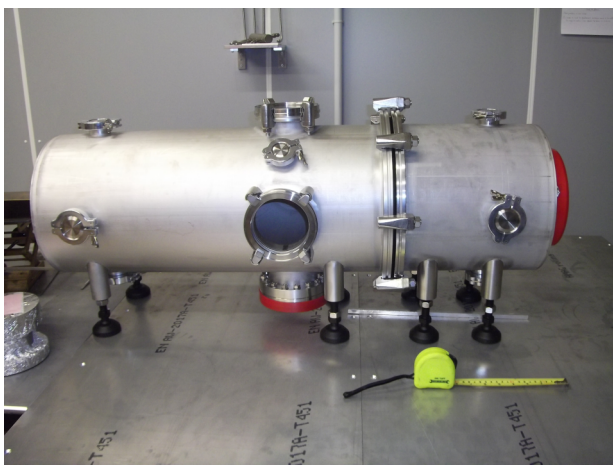

FIG. 2. Picture of the vacuum chamber.

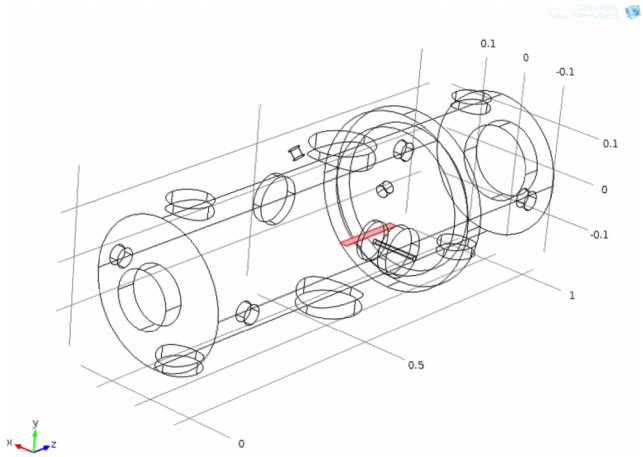

FIG. 3. 3D drawing of the Aline chamber with its 15 ports, the antenna position in the middle port and the potential map area corresponding to maps of the 3rd section.

(0.1 ohm measured) and their theoretical inductance is 4.2 mH. The magnetic ripple remains lower than 5% (see Figure 5) and allows multiple electron or ion cyclotron resonance layers along the chamber. For 200 A, the coils can dissipate 24 kW of Joule power evacuated by a 6 l/min water flux per coil with a temperature increase of 20° between the inlet and the outlet. To match this flux, a 12 bars pressure is required at intake according to the measured fluid resistance of each coil. The measured fluid resistance at a flow rate of 2 l/min is 8×10^9 Pa s/m^{-3}, which is 2.5 higher than the laminar Poiseuille theory (3×10^9 Pa s/m^{-3}) as the flow starts to be turbulent at a flow rate of 1 l/min. These coils are fed with three 15 kW power sources PS 8000 3U made by Elektro-Automatik and able to produce a DC current from 0 to 510 A between 0 and 80 V. Each power supply is connected to a pair of coils in series enabling the longitudinal modulation of the magnetic field. The power supplies are coupled to a temperature controller on each coil so that they can be switched off in case of overheating and thus avoid the melting of the PVC layer on the copper tubes.

E. The RF amplifier

One of the most relevant components of all this machinery is the broadband RF amplifier Prana DP 600 made by Prana

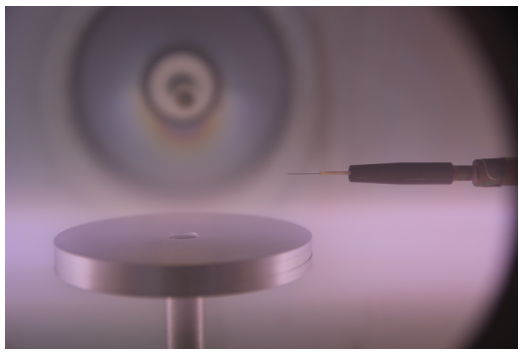

FIG. 4. Picture of the compensated probe head above the RF antenna disc. The collector is the small tungsten tip at the end of the main body.

This article is copyrighted as indicated in the article. Reuse of AIP content is subject to the terms at: http://scitationnew.aip.org/termsconditions. Downloaded to IP: 193.50.135.4 On: Fri, 30 Oct 2015 10:16:52

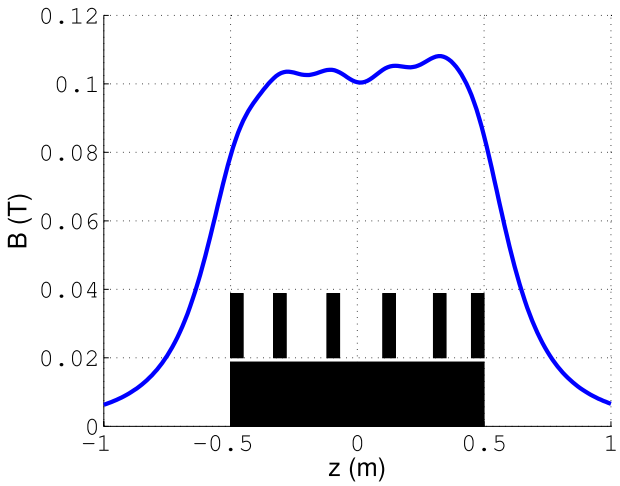

FIG. 5. Magnetic field distribution along the main axis of the cylindrical chamber for a 200 A current per coil.

Corporation. Its nominal power is close to 600 W but can rise up to 1100 W in the 1 MHz range. The bandwidth is in the range 10 kHz to 250 MHz allowing a wide number of wave cutoff and resonances testing in the plasma. This amplifier is connected to a coupler able to measure both forward and reflected powers flowing along the coaxial cable feeding the antenna in the plasma chamber. The amplifier is designed to support up to 400 W of reflected power and does not need to be matched to keep working. It can launch half of its maximum power even for an infinite SWR (Standing Wave Ratio).

F. The antenna

The RF antenna is a capacitive aluminum disc (8 cm in diameter and 10 mm thick) located in the middle of the chamber along the z axis and 7 cm far from chamber center. The antenna could be an inductive loop as well. The main advantage of this 2 parts chamber is to easily change the type of antenna and test various configurations. The typical ICRF antenna in tokamaks is made by current straps, which means an inductive coupling for frequencies around 50 MHz. In Aline, the magnetic field is 30 times lower (0.1 T) than in the edge of tokamaks and then the ion cyclotron frequency is much lower (from 40 kHz to 1 MHz) depending on the gas injected (H, D, He, and Ar). The present capacitive antenna should be replaced soon by an inductive one to launch a magnetosonic wave into the plasma.[28]

G. Pressure regulation

The pressure is monitored by 2 pressure gauges. The first one is a Pirani gauge working between the atmospheric pressure and 10^{-4} mbar, and the second one is a cold cathode gauge working between 10^{-2} and 10^{-9} mbar. The pressure is controlled via 2 flowmeters able to inject 2 gases simultaneously. In addition, a motorized butterfly valve between the turbo-pump and the chamber adjusts the suction aperture to minimize the gas influx. In Aline, the typical working pressure ranges from 10^{-3} mbar to 10^{-1} mbar.

III. PHYSICS INVOLVED IN ALINE

A. Magnetic point of view

This experimental reactor has been designed to study strongly magnetized plasma and its heating via RF waves, including RF power coupling and RF sheaths. Therefore, the device must be able to excite ion cyclotron resonance as it is done in tokamaks and to confine thermal ions within the plasma chamber. The magnetic coils can produce a field of about 0.1 T, which corresponds to a Larmor radius of 3×10^{-2} mm at $T_e = 2$ eV for electrons and 1 mm radius for cold argon ions. The plasma is considered as strongly magnetized as thermal ion, i.e., 2 eV Ar ions, still have a centimetric Larmor radius, much smaller than the 30 cm diameter of the cylindrical chamber.

B. Main plasma characteristics

The electrical behaviour of the plasma is modelled by its dielectric tensor, derived from the conductivity tensor obtained from the fluid motion equation, the mass conservation, and Poisson equation, respectively.

The electron to ion mobility ratio is given by $\sqrt{m_i/m_e}$ in the parallel direction and scales with the Larmor radius in the perpendicular one, giving a larger mobility for ions. As a consequence, in typical capacitively coupled discharges in a 0.1 T magnetic field, the conductivity along the magnetic lines is several orders of magnitude larger than the perpendicular ones. The parallel ion acceleration and the perpendicular electron motion can be neglected in most modelings. Another important parameter in plasma discharges is the collision frequency ν_{eN} between electrons and neutrals and ν_{iN} for ions and neutrals. The plasma ionization rate is rather small ($\approx 1/1000$) so that neutral density N is of order 10^{20} m^{-3}. As a consequence, the cold plasma tensor can be refined with this collision frequency. In order to consider electrons and ions as magnetized, their collision frequency must be lower than the cyclotron frequency or, in other words, the mean free path for ions λ^i_{mfp} and electrons λ^e_{mfp} must be larger than their Larmor radii. Last but not least, the plasma breakdown relies on an avalanche ionization process that requires a mean free path much lower than the size of the chamber. Under these considerations, the targeted main plasma parameters are given in Table I.

C. RF waves

The RF waves in such a metric chamber are mainly electrostatic, which means their wavelength is much larger than the typical size of the plasma. The wave theory can be derived from the cold plasma tensor, which yields the basic electric behavior of a cold magnetized plasma. In this tensor, many characteristic frequencies appear such as the electron and ion cyclotron resonant frequencies ω_{ce} and ω_{ci} , the ion and electron plasma cutoff frequencies ω_{pe} and ω_{pi}, and the hybrid frequencies which are a combination of them. All of these frequencies can be excited by the RF amplifier considering the wide range of plasma parameters.

This article is copyrighted as indicated in the article. Reuse of AIP content is subject to the terms at: http://scitationnew.aip.org/termsconditions. Downloaded to IP: 193.50.135.4 On: Fri, 30 Oct 2015 10:16:52

TABLE I. Typical plasma parameters expected in the Aline RF plasma device at B = 0.1 T.

Gas	Argon	Helium
$n_i = n_e$ (m^{-3})	$10^{15} \rightarrow 10^{17}$	…
N (m^{-3})	$10^{20} \rightarrow 10^{21}$	…
T_e (eV)	$1.5 \rightarrow 2$	…
T_i (eV)	0.026	…
$\omega_{pi}/2\pi$ (Hz)	$10^6 \rightarrow 10^7$	$3 \times 10^6 \rightarrow 3 \times 10^7$
$\omega_{pe}/2\pi$ (Hz)	$3 \times 10^8 \rightarrow 3 \times 10^9$	…
$\omega_{ci}/2\pi$ (Hz)	4×10^4	4×10^5
$\omega_{ce}/2\pi$ (Hz)	2.8×10^9	…
ν_{iN} (Hz)	$10^4 \rightarrow 10^5$	$10^4 \rightarrow 10^5$
ν_{eN} (Hz)	$6 \times 10^5 \rightarrow 6 \times 10^7$	…
r_L^i (mm)	1	0.3
r_L^e (mm)	0.03	…
λ_{De} (mm)	$0.3 \rightarrow 0.03$	…
λ_{mfp}^i (mm)	$2 \rightarrow 20$	$5 \rightarrow 50$
λ_{mfp}^e (m)	$0.01 \rightarrow 1$	…

D. RF sheath physics

The last important aspect is the sheath dynamics, especially the RF sheath physics in front of the RF antenna. To make measurements in the sheath, this one must be larger than 1 mm according to the probe tip width (0.15 mm) to accurately resolve this region. And the motorized manipulator accuracy must be smaller than the probe diameter, which is the case here. The sheath width scales as $\lambda_{De}.(V_{rf}/T_e)^{3/4}$. For V_{rf} = 400 V, T_e = 1 eV, and plasma density of 10^{16} m^{-3}, the sheath width is equal to 6 mm, which makes the potential profile measurement possible in the sheath. Under an applied magnetic field, the perpendicular sheath dynamics is not well known and has to be studied experimentally with RF waves to build analytical models.

IV. TYPICAL PLASMA PARAMETERS AND FIRST RESULTS WITHOUT MAGNETIC FIELD

A. Plasma parameters and density map

The unmagnetized plasma parameters expected in Aline reactor can be evaluated by the analytical "global model" built by Lieberman[9–11] and Chabert[14] and compared to reference results.[15–17] Considering the same discharge parameters as for measurements in Aline (Table II), the densities expected for the $10^{-2} - 5 \times 10^{-1}$ mbar argon pressure range from 5×10^{14} to 5×10^{16} m^{-3}.

TABLE II. Argon plasma parameters for Figures 8, 9, and 10.

Gas	Argon
Forward RF power	24 W
Frequency	40 MHz
Pressure	2×10^{-2} mbar
T_e range	1.5–2 eV
T_i	0.026 eV

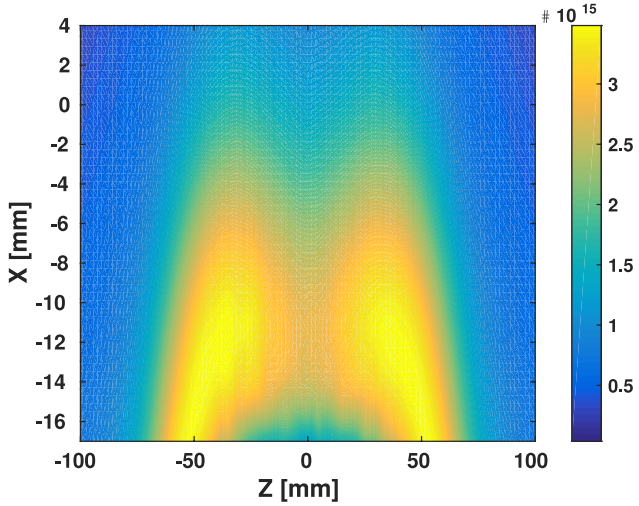

FIG. 6. Ion density map computed from the plasma module in *Comsol* software. The density magnitude is given by the colorbar and is expressed in m^{-3}.

These densities and electron temperature are confirmed by a 2D Comsol[19] simulation of the chamber cross section of Aline reactor as it can be seen in Figure 6 for the same discharge parameters. This simulation has been achieved with the plasma module[19–21] taking into account collisions between electrons, ions, and neutrals, ionization rate per species, and a diffusion equation per species coupled to an electrostatic potential resolution.

B. Probe measurement protocol

Measurements have been achieved with the self-compensated Langmuir probe which can be biased by using an external control box. The probe bias varies from −70 V to 70 V but only the values above −20 V have been plotted in Fig. 7(a). This potential range allows for sweeping across a typical

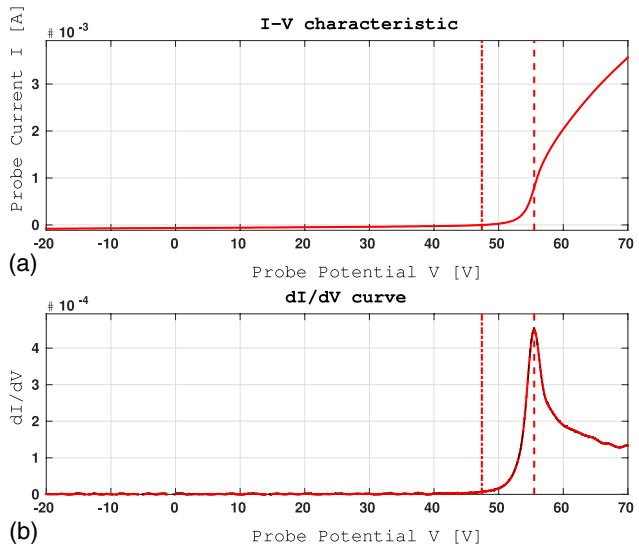

FIG. 7. I-V characteristic ((a)—top) and its first derivative ((b)—bottom) obtained from a RF-compensated Langmuir probe. Floating potential is derived from point at which the total current is zero; plasma potential is derived from the maximum of the first derivative.

This article is copyrighted as indicated in the article. Reuse of AIP content is subject to the terms at: http://scitationnew.aip.org/termsconditions. Downloaded to IP: 193.50.135.4 On: Fri, 30 Oct 2015 10:16:52

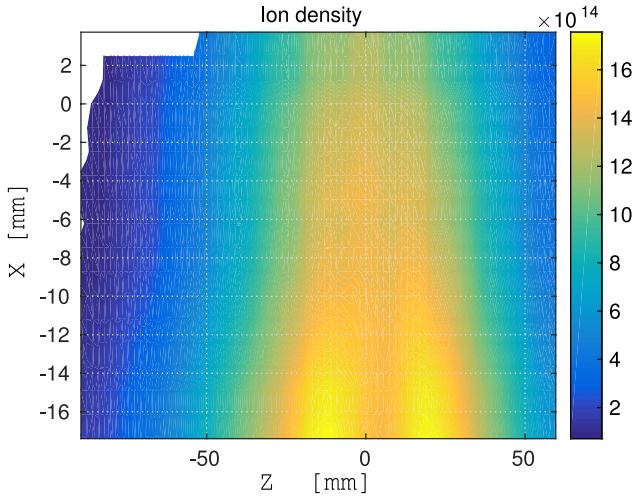

FIG. 8. Ion density map probed in front of the RF antenna. The density magnitude is given by the colorbar and is expressed in m^{-3}.

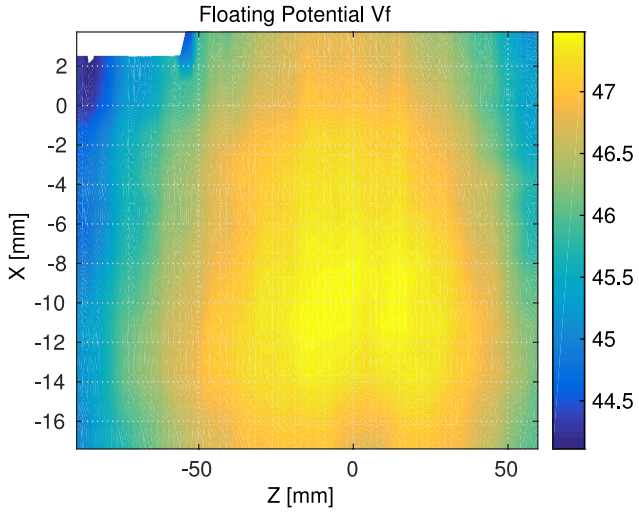

FIG. 9. Floating potential map in front of the RF antenna centered on Z = 0. The antenna diameter is 8 cm. The floating potential magnitude is given by the colorbar and is expressed in Volts.

current-voltage probe characteristic derived from an argon discharge at 10^{-2} mbar, 25 W input power, and 40 MHz RF, as shown in Fig. 7(a).

The ion saturation current is found on the left part of the curve and the electron contribution to the right. The floating potential V_f corresponds to the potential for which the ion and electron currents collected by the probe are equal, so that the total current measured is zero. The zoom enclosed in the figure focuses on the floating potential V_f area. Even if the averaging process provides a very clean curve (black curve), this one is smoothed (red curve) with a Savitzky-Golay algorithm in order to improve the determination of V_f. The accuracy of the value provided by the algorithm is found to be better than 0.1 V. The plasma potential V_p (sometimes called space potential) is derived from the point of the curve where it starts to deviate from the exponential growth.[18] The most reliable way to determine it has been found to be the search for the maximum of the I-V characteristic first derivative. The curve corresponding to the above example is given in Figure 7(b). The determination of n_i consists in measuring the ion saturation current equal to $e.n_i.C_s$, with C_s the ion acoustic velocity by biasing the probe tip negatively. As for the electron density n_e, it is deduced from the exponential part of the I-V curve considering Boltzmann electrons. The electron temperature is retrieved from the same part of the I-V curve: the slope of the I-V curve is proportional to T_e when the current is null. These techniques have been improved and are known as the Orbital Motion Limited (OML) theory[3] applied here to the specific case of a cylindrical probe.

The different curves obtained are smooth and do not exhibit unexpected features such as, for instance, multiple maxima for dI/dV. An algorithm can then be applied in order to automatically determine these parameters, so that the several hundred measurements required for 2D and 3D maps can be processed in a reasonable amount of time and clicks.

C. Experimental maps

In Figs. 8, 9, and 10 are given 2D maps of ion density n_i (Figure 8), floating potential V_f, and plasma potential V_p, respectively. They have been experimentally derived from I-V characteristic such as the one presented previously. The discharge parameters are shown in Table II.

For these maps, data have been taken every 1.2 mm in the x direction and 1.9 mm in the z direction. Floating potential, plasma potential, ion density, and electron temperature are derived for each of them. In Figures 8, 9, and 10, the RF antenna lies between x = −40 mm and +40 mm, at z ≈ −18 mm.

The first analysis showed a density up to 5×10^{15} m^{-3} for electrons and 3 times lower for ions (Figure 8). The methods to retrieve ion and electron density[3] come from 2 different parts of the I-V characteristics and lead to such discrepancies. The reliability of the method to retrieve the ion density depends strongly on the possible current shift of the characteristics.[12,13]

In Figure 9 is shown an example of a 2D floating potential map plotted still using the probe acquisitions. This map exhibits a floating potential quite constant over several centimeters around the antenna. In the same way, the plasma potential

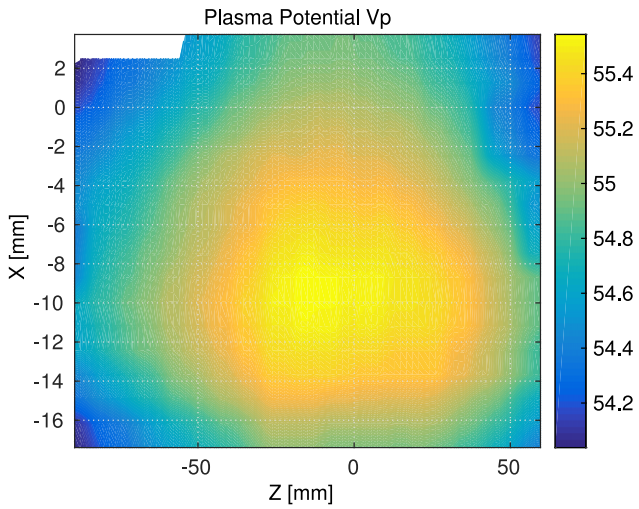

FIG. 10. Plasma potential map in front of the RF antenna. The floating potential magnitude is given by the colorbar and is expressed in Volts.

This article is copyrighted as indicated in the article. Reuse of AIP content is subject to the terms at: http://scitationnew.aip.org/termsconditions. Downloaded to IP: 193.50.135.4 On: Fri, 30 Oct 2015 10:16:52

remains constant in front of the antenna and is several volts higher than the floating potential as expected according to the theory (Figure 10).

D. Comparison of density maps

Experimental (Fig. 8) and Comsol density maps (Fig. 6) show a fair agreement when comparing the spatial extent of the plasma. Both densities peak at similar values, 1.6×10^{15} m^{-3} and 3×10^{15} m^{-3}, respectively. This is quite a satisfactory result as the discrepancy lies well within the experimental error bars related to ion density measurement, estimated so far at one order of magnitude. The RF potential in the Comsol simulations is 250 V, which is higher than in the experiment and can explain the higher density obtained by using COMSOL software. Nevertheless, this demonstrates that COMSOL could be a confident way to forecast the density and temperature expected in the experiments, at least regarding the order of magnitudes. In the same way, the temperature map has been obtained in COMSOL but is not represented here because the electron temperature is rather constant in front of the antenna and close to 2 eV as measured by the probe.

E. Series resonances

One of the most interesting results during this first experimental campaign is the highlighting of the series resonances[14] by a frequency sweep of the RF power in the reactor Aline for parameters appearing in Table III. S_2 and S_1 are, respectively, the area of the grounded wall chamber and the RF antenna. V_{rf} is the potential applied on the antenna. This potential is deduced from the coupler measurement and takes into account the 50 cm length of the cable between the antenna and the coupler.

The coupler connected between the antenna and the RF amplifier measures the forward and reflected potentials as a function of the frequency. At these resonances, the reflected power is much lower and depends on the combined impedance of the plasma and the coaxial cable connected between the amplifier and the antenna. The plasma chamber impedance Z_p plotted in Figure 11 can be deduced from the reflection coefficient Γ measured by the coupler as follows: $Z_p = Z_g.(1 + \Gamma)/(1 - \Gamma)$.

One can see that 3 resonances appear, two of them come from the cable itself and one from the plasma chamber (including plasma core, sheath, wall, and antenna). These resonances are series resonances due to a matching of the RF wavelength with the electrical length of the whole system (plasma chamber + coaxial cable + internal amplifier impedance). The coaxial

TABLE III. Plasma parameters for impedance plots in the unmagnetized plasma.

Gas	He
Pressure	3.3 Pa
S_2/S_1	100
V_{RF}	50 → 150 V
RF power	≈60 W

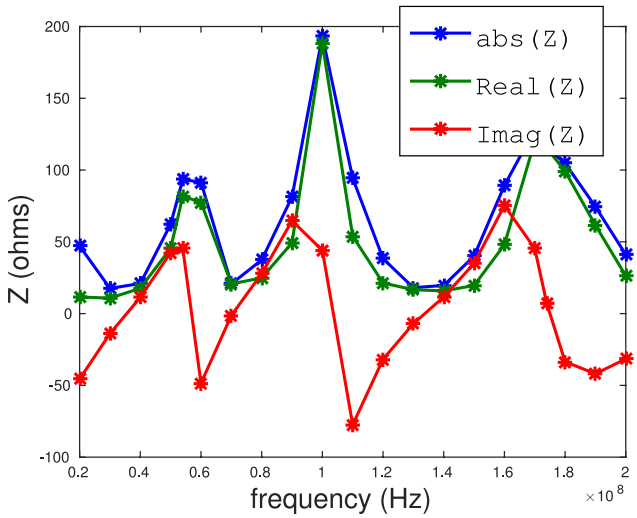

FIG. 11. Plasma + chamber + cable impedance in reactor Aline as a function of the frequency.

cable impedance (type RG 213-U) is known (50 Ω) so that the phase shift induced can be evaluated.[22] The reflection coefficient Γ is shifted due to the cable length: $\Gamma_s = \Gamma.\exp(2i\beta z)$, with $\beta = \omega/v$, ω the RF pulsation and v (=0.66 c) the speed of light in the coaxial cable, and z (=0.5 m) is the cable length.

By subtracting the cable shift contribution (and supposing no absorption in the good conductor cable), one retrieves the plasma + chamber + antenna impedance (Figure 12) that can be used to identify the plasma resonance.

A good evaluation of the plasma density can be obtained from the peak resonance which simply equals the plasma pulsation ω_{pe}.[14] This plasma density here is equal to 9×10^{13} m^{-3} for the plasma parameters in Table III.

F. Plasma impedance model

Using Lieberman's model for the core plasma, and an equivalent impedance for the sheath in front of the antenna

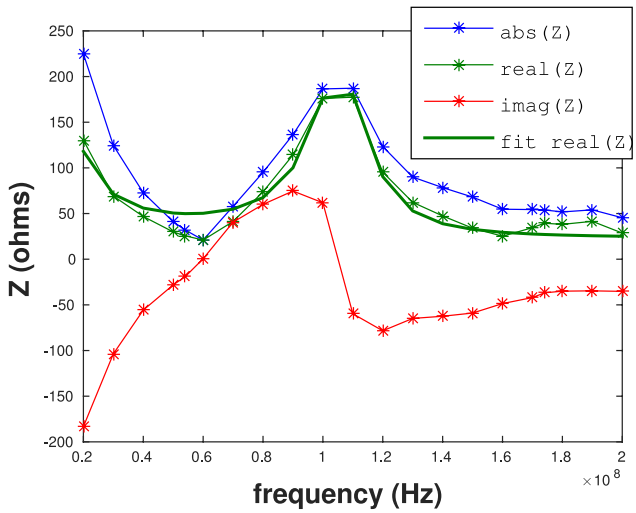

FIG. 12. Plasma + chamber impedance in reactor Aline as a function of the frequency. The real part of the impedance is fitted by the analytical model based on the electric circuit in Figure 13.

This article is copyrighted as indicated in the article. Reuse of AIP content is subject to the terms at: http://scitationnew.aip.org/termsconditions. Downloaded to IP: 193.50.135.4 On: Fri, 30 Oct 2015 10:16:52

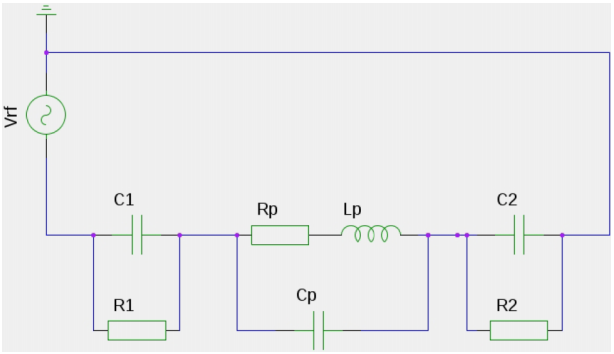

FIG. 13. Equivalent electric model of the plasma and sheaths.

associated to the grounded wall of the chamber (electric sketch on Figure 13), one can fit the experimental impedance curve with the expected one (Figure 12).

In this model, the plasma density is assumed to be constant for any frequency and the sheath impedance is treated as a capacitor in parallel with an equivalent resistor corresponding to one working point of the non-linear IV characteristics.[23,24] The sheath capacitances C_1 and C_2 are given by Lieberman[26] and the sheath resistances R_1 and R_2 are calculated according to the strong asymmetry between the grounded wall and the antenna surface.

Actually, the current collected on the antenna is mainly electronic because of the self-biasing between the plasma core and the antenna. The average potential drop in the RF sheath[25] on the antenna side is thus much higher than on the grounded wall side. For an infinite asymmetry, this average potential drop can tend to V_{rf}, the amplitude of the RF potential on the antenna.[9] As a consequence, and due to the strongly non-linear I-V characteristic of the sheath, the current collected is close to the ion saturation current on the grounded wall side. The equivalent sheath resistance on the antenna side is then

$$R_1 = V_{rf}/(j_i.S_2).$$

The sheath impedance in front of the grounded wall can be taken equal to the one in front of the antenna ($R_1 = R_2$) because of the current conservation, supposing a low resistive plasma ($R_p \ll R_1$). The plasma and amplifier internal resistance are much lower than the sheath resistance. This is not always the case and a more refined model is necessary. This model especially designed for asymmetric and unmagnetized discharge will be presented in a forthcoming paper and will be based on a former work on double probe.[27] The global approach proposed by Lieberman leads to the impedance for the sheath as $Z_{sh} = R_1./(1 + i.R_1.C_1.w) + R_2./(1 + i.R_2.C_2.w)$ and the impedance for the plasma as $Z_p = 1./(1./(R_p + i.Lp.w) + i.C_p.w)$.

According to the simplicity of the model, the best matching occurs for the equivalent impedances appearing in Table IV and corresponding to the equivalent electric circuit presented in Figure 13. For these parameters, the real part of the impedance is really well fitted in Figure 12.

From these impedances, one can deduce the typical plasma parameters of the discharge in Table V. The density obtained by the impedance method is the average density in the whole chamber and is in the same order as the one given by the global model from Lieberman and comparable to experimental reference results.[15–17] No probe measurements were available at this time to confirm these results in helium because the I-V characteristics were not easily interpretable. A double slope appears in the exponential region of the characteristics making the evaluation of T_e difficult. In addition, the model should be refined by considering a variation of the plasma density as a function of the coupled power, which depends highly on the frequency. Nevertheless, this first raw approach is quite satisfactory and yields a good evaluation of each order of magnitude of the plasma parameters.

TABLE IV. Equivalent impedances for the plasma model (Figure 13) fitting the real part of the plasma impedance in Figure 12.

R_1	13 111 Ω
R_2	102 008 Ω
C_1	8.9×10^{-12} F
C_2	1.1×10^{-11} F
R_p	16.7 Ω
L_p	8.1×10^{-8} H
C_p	2.7×10^{-11} F

V. PROSPECTS AND SCIENTIFIC TASKS

These first experiments' series have shown that it was possible to map the floating potential around the RF antenna with a good accuracy, which made possible the deduction of the plasma parameters using well adapted model. The forthcoming tasks will be dedicated to in-depth studies of the sheath and presheath configuration in the presence of a magnetic field and to the effect of the antenna geometry on the plasma parameters. These studies are detailed in Sec. V A–V C.

A. Perpendicular conductivity of the plasma and sheath in a magnetized plasma

The perpendicular lengths of potential structures in the plasma depends directly on the transverse conductivity of the plasma. The simplest form for this plasma conductivity is given by the dielectric tensor of a cold plasma.[28] 3D Comsol simulations can already compute the DC potential distribution in Aline (see Figure 14) with simple sheath boundary conditions and a cold dielectric tensor in the core plasma.

Thanks to the comparison between computed and experimental maps, we will be able to conclude about the assumption of cold plasma and if a collisional term should be added. Other analytical and fluid models, also available in the literature,[5,29–32] will be especially benchmarked to check the rectified sheath potential as a function of the RF voltage and plasma parameters.[27]

TABLE V. Plasma parameters deduced from the fit of the real part of the plasma impedance in Figure 12.

Gas	He
n_0	10^{14} m^{-3}
T_e	5 eV
ν_m	2×10^8 s^{-1}

This article is copyrighted as indicated in the article. Reuse of AIP content is subject to the terms at: http://scitationnew.aip.org/termsconditions. Downloaded to IP: 193.50.135.4 On: Fri, 30 Oct 2015 10:16:52

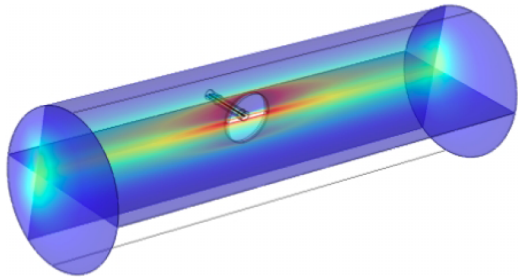

FIG. 14. *Comsol* DC potential map in a magnetized plasma in Aline reactor.

One of the main unknown is the sheath equivalent capacitance when the magnetic field is tilted with respect to the wall or in the extreme case when this tilt tends to zero. The experimental work and dedicated PIC (particle in cell) codes[33] would help finding the best model to input as a boundary condition in Comsol simulation. For now, the transverse conductivity of the sheath in Comsol models is the same as the plasma conductivity.

B. Propagation of non-linear plasma waves as a function of the magnetic field

The theory of waves in plasmas is often restricted to linear theory preventing low frequency waves to propagate in a too dense plasma. Solitary waves induced by the strong potential on the antenna could propagate through the plasma, just as in the SOL of tokamak near ICRF antenna. It has been observed that ICRF shots strongly increase the plasma transport in the SOL. The propagation of such solitary waves all around the edge of the torus is likely to be another candidate to explain this anomalous perpendicular transport.[34] This can be diagnosed via reflectometry.[35]

C. Testing of different antenna designs able to mitigate sheath potentials and improve ICRF heating efficiency

The building of such test bed was initiated in the way to test the validity of our RF sheath and ICRF antenna models.[36,37] A similar test bed was built at IPP Garching under the name "Ishtar." This experimental tool is composed of a 1 MW ICRF antenna launching the wave in a plasma under a 0.1 tesla magnetic field. Ishtar is more oriented toward high power ICRF antenna in magnetic fusion plasmas, while Aline is dedicated to low power RF sheath + antenna physics in cold plasmas. Finally, both experiments are complementary and allow a wide exploration of the ICRF heating.

Obviously, the RF power in Aline is far smaller than for ICRF tokamak antenna (several MW). The purpose here is to test different designs (square, round shapes, conductor combined with dielectric) and coupling (capacitive, inductive, or both). On the other hand, the low RF power allows the building of low cost antenna with new designs to be tested. The capacitive coupling is not the best way to efficiently transfer the RF power to the plasma because the electric field must be high enough and arcing is likely to occur. A more efficient way is to choose an inductive coupling with a coil antenna minimizing electric field and thus sheath potentials close to the antenna but inducing strong electric currents in a small layer in the edge of the plasma. The coupling efficiency can still be measured with the coupler connected between the amplifier and the antenna.

Finally, the main goal of this antenna is to heat ions by launching an ion cyclotron wave crossing a resonance layer whose thickness depends on the magnetic field gradient. This ion cyclotron wave can be electrostatic or electromagnetic (fast wave) and can propagate across the magnetic field[38] to be absorbed in the resonant layer. All these aspects could be diagnosed with the Langmuir probe. In addition, we should be able to make minority heating as it is made in tokamaks because the reactor is equipped with 2 flowmeters allowing the injection of 2 gases simultaneously.

VI. CONCLUSION

Aline is a new cylindrical plasma discharge reactor, whose main purpose is to study RF sheath during ICRF heating. This low RF power experiment is diagnosed to draw 3D map of the floating potential, the plasma potential, ion density, electron density, and electron temperature using a simple RF self-compensated probe mounted on a motorized manipulator. The comparison between these unmagnetized experimental results and both analytical models and COMSOL simulations shows a very good agreement. The next step of experimental studies is to investigate the effect of the magnetic field, to approach the edge plasma parameters of tokamaks for which the analytical double probe model has been first built. These "magnetized maps" will allow the drawing of the 3D convection map of the plasma, in the way to deduce the heat fluxes supported by the antenna structure. The main goal is to check the validity of the assumptions made in our fluid double probe models with perpendicular conductivity. The next step will be to optimize the antenna design to mitigate the average potential in front of the antenna, which results in a mitigation of convection and turbulent transport. The easily reconfigurable design of the chamber offers the possibility to study other phenomena like solitary waves and current collected by different parts of the chamber as a function of the self-biasing and the magnetic field magnitude.

ACKNOWLEDGMENTS

Financial support was received from the French National Research Agency through Contract No. ANR-12-JS09-0013-01 SPICE RF. The authors acknowledge as well the ANR *PEPPSI* Project (No. ANR-12-BS09-028-01) for supporting the probe. This work, supported by the European Communities under the contract of Association between EURATOM, CEA and the French Research Federation for fusion studies, was carried out within the framework of the European Fusion Development Agreement.

[1]J.-M. Noterdaeme and G. Van Oost, Plasma Phys. Controlled Fusion **35**, 1481-1511 (1993).
[2]P. C. Stangeby, *The Plasma Boundary of Magnetic Fusion Devices* (Institute of Physics Publishing, Bristol and Philadelphia, 2000), p. 369.
[3]F. F. Chen, Plasma Sources Sci. Technol. **18**, 035012 (2009).

This article is copyrighted as indicated in the article. Reuse of AIP content is subject to the terms at: http://scitationnew.aip.org/termsconditions. Downloaded to IP: 193.50.135.4 On: Fri, 30 Oct 2015 10:16:52

[4]E. Faudot, S. Heuraux, and L. Colas, Phys. Plasmas **13**, 042512 (2006).
[5]E. Faudot, S. Heuraux, M. Kubic, J. Gunn, and L. Colas, Phys. Plasmas **20**, 043514 (2013).
[6]P. A. Chatterton, J. A. Rees, W. L. Wu, and K. Al-Assadi, Vacuum **42**(7), 489-493 (1991).
[7]J. Gunn *et al.*, IAEA 2008, EX/P6-32.
[8]M. Kubic, "Measurement of sheath potential in RF-biased flux tubes using a retarding field analyzer in Tore Supra tokamak," in *PSI Proceedings* (PSI, 2012), pp. 1-60.
[9]M. A. Lieberman and A. J. Lichtenberg, *Principles of Plasma Discharges and Materials Processing*, 2nd ed. (John Wiley and Sons, INC Publication, 2005).
[10]M. A. Lieberman and R. A. Gottscho, in *Physics of Thin Films*, edited by M. Francombe and J. Vossen (Academic, New York, 1994), Vol. 18, p. 139.
[11]C. Lee, D. B. Graves, M. A. Lieberman, and D. W. Hess, "Global model of plasma chemistry in a high density oxygen discharge," J. Electrochem. Soc. **141**, 1546 (1994).
[12]J. D. Swift and M. J. R. Schwar, *Electrical Probes for Plasma Diagnostics* (Iliffe, London, 1970).
[13]A. Boschi and F. Magistrelli, II Nuovo Cimento **29**, 487 (1963).
[14]P. Chabert and N. Braithwaite, *Physics of Radio-Frequency Plasmas* (Cambridge University Press, 2011).
[15]D. Lymberopoulos and D. Economou, J. Res. Natl. Inst. Stand. Technol. **100**, 473 (1995).
[16]K. Dzierzega, K. Musiol, E. C. Benck, and J. R. Roberts, J. Appl. Phys. **80**, 3196 (1996).
[17]J. Olthoff and K. Greenberg, J. Res. Natl. Inst. Stand. Technol. **100**, 327 (1995).
[18]F. F. Chen, Phys. Plasmas **9**(4), 1449 (2002).
[19]COMSOL, The Plasma Module User Guide, 2011.
[20]COMSOL, GEC CCP Reactor, Argon Chemistry, 2011.
[21]COMSOL, Benchmark Model of a Capacitively Coupled Plasma, 2012.
[22]A. Vander Vorst, *Transmission, Propagation et Rayonnement* (De Boeck Universit, Bruxelles, 1995).
[23]M. A. Sobolewski, Appl. Phys. Lett. **70**, 1049 (1997).
[24]M. A. Sobolewski, Appl. Phys. Lett. **72**(10), 1146 (1998).
[25]A. Godyak and A. A. Kuzovnikov, Fiz. Plazmy **1**, 496-503 (1975) [Sov. J. Plasma Fiz. **1**, 276 (1975)].
[26]M. A. Lieberman, IEEE Trans. Plasma Sci. **17**(2), 338-341 (1989).
[27]E. Faudot, L. Colas, S. Heuraux, and J. P. Gunn, Phys. Plasmas **17**, 042503 (2010).
[28]T. H. Stix, *Waves in Plasmas*, 2nd ed. (American Institute of Physics, 1992).
[29]V. A. Rozhansky, S. P. Voskoboynikov, E. G. Kaveeva, D. P. Coster, and R. Schneider, Nucl. Fusion **41**(4), 387-401 (2001).
[30]A. V. Nedospasov and D. A. Uzdensky, Contrib. Plasma Phys. **34**, 478 (1994).
[31]A. Carlson, Phys. Plasmas **8**, 4732 (2001).
[32]A. Ngadjeu, E. Faudot, L. Colas, S. Heuraux, J. Gunn, and M. Kubic, J. Nucl. Mater. **415**, S1009-S1012 (2011).
[33]C. K. Birdsall and A. B. Langdon, *Plasma Physics via Computer Simulation* (McGraw-Hill, New York, 1985).
[34]Ph. Ghendrih, Y. Sarazin, G. Attuel, S. Benkadda, P. Beyer, G. Falchetto, C. Figarella, X. Garbet, V. Grandgirard, and M. Ottaviani, Nucl. Fusion **43**, 1013-1022 (2003).
[35]G. Hornung, F. Clairet, G. L. Falchetto, R. Sabot, H. Arnichand, and L. Vermare, Plasma Phys. Controlled Fusion **55**, 125013 (2013).
[36]L. Colas *et al.*, Nucl. Fusion **45**, 767-782 (2005).
[37]M. L. Garrett, "Mitigation of rf sheaths through design and implementation of magnetic field-aligned icrf antenna," Ph.D. thesis (MIT, 2012).
[38]D. G. Swanson, *Plasma Waves*, 2nd ed. (IOP Publishing Ltd, 2003).

This article is copyrighted as indicated in the article. Reuse of AIP content is subject to the terms at: http://scitationnew.aip.org/termsconditions. Downloaded to IP: 193.50.135.4 On: Fri, 30 Oct 2015 10:16:52